Cell Reports

Accelerating Novel Candidate Gene Discovery in Neurogenetic Disorders via Whole-Exome Sequencing of Prescreened Multiplex Consanguineous Families

Graphical Abstract

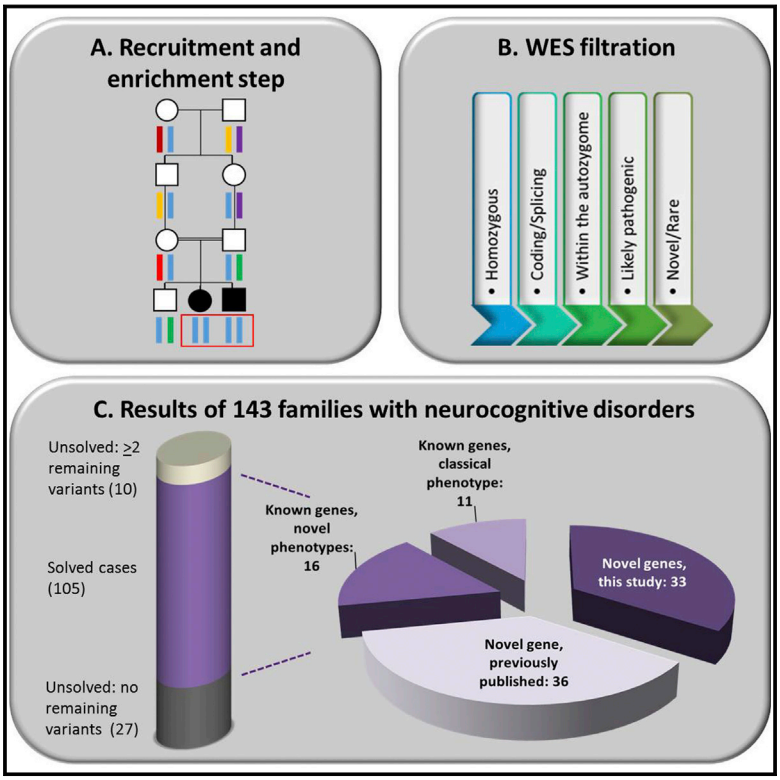

Highlights

- Multiplex consanguineous families are rich sources for novel gene discovery
- Prescreening these families for known disease genes accelerates gene discovery
- 33 novel candidate genes are reported in this study

Authors

Anas M. Alazami, Nisha Patel, ..., Dorota M. Monies, Fowzan S. Alkuraya

Correspondence

falkuraya@kfshrc.edu.sa

In Brief

Using whole-exome sequencing on prescreened multiplex consanguineous families, Alazami et al. describe the identification of 33 novel candidate genes for various neurogenetic conditions. Such families are rich sources for novel gene discovery.

Alazami et al., 2015, Cell Reports *10*, 148–161
January 13, 2015
http://dx.doi.org/10.1016/j.celrep.2014.12.015

OPEN ACCESS
CellPress

Cell Reports
Report

Accelerating Novel Candidate Gene Discovery in Neurogenetic Disorders via Whole-Exome Sequencing of Prescreened Multiplex Consanguineous Families

Anas M. Alazami,[1,23] Nisha Patel,[1,23] Hanan E. Shamseldin,[1,23] Shamsa Anazi,[1] Mohammed S. Al-Dosari,[2] Fatema Alzahrani,[1] Hadia Hijazi,[1] Muneera Alshammari,[3] Mohammed A. Aldahmesh,[1] Mustafa A. Salih,[3] Eissa Faqeih,[4] Amal Alhashem,[5,6] Fahad A. Bashiri,[3] Mohammed Al-Owain,[5,7] Amal Y. Kentab,[3] Sameera Sogaty,[8] Saeed Al Tala,[9] Mohamad-Hani Temsah,[3] Maha Tulbah,[10] Rasha F. Aljelaify,[11] Saad A. Alshahwan,[6] Mohammed Zain Seidahmed,[12] Adnan A. Alhadid,[3] Hesham Aldhalaan,[13] Fatema AlQallaf,[13] Wesam Kurdi,[10] Majid Alfadhel,[14] Zainab Babay,[15] Mohammad Alsogheer,[16] Namik Kaya,[1] Zuhair N. Al-Hassnan,[5,7] Ghada M.H. Abdel-Salam,[17] Nouriya Al-Sannaa,[18] Fuad Al Mutairi,[14] Heba Y. El Khashab,[3,19] Saeed Bohlega,[13] Xiaofei Jia,[20] Henry C. Nguyen,[20] Rakad Hammami,[1] Nouran Adly,[1] Jawahir Y. Mohamed,[1] Firdous Abdulwahab,[1] Niema Ibrahim,[1] Ewa A. Naim,[1,21] Banan Al-Younes,[1,21] Brian F. Meyer,[1,21] Mais Hashem,[1] Ranad Shaheen,[1] Yong Xiong,[20] Mohamed Abouelhoda,[1,21] Abdulrahman A. Aldeeri,[1,22] Dorota M. Monies,[1,21] and Fowzan S. Alkuraya[1,5,21,*]

[1]Department of Genetics, King Faisal Specialist Hospital and Research Center, Riyadh 11211, Saudi Arabia
[2]Department of Pharmacognosy, College of Pharmacy, King Saud University, Riyadh 11451, Saudi Arabia
[3]Department of Pediatrics, King Khalid University Hospital and College of Medicine, King Saud University, Riyadh 11451, Saudi Arabia
[4]Department of Pediatrics, King Fahad Medical City, Riyadh 11525, Saudi Arabia
[5]Department of Anatomy and Cell Biology, College of Medicine, Alfaisal University, Riyadh 11533, Saudi Arabia
[6]Department of Pediatrics, Prince Sultan Military Medical City, Riyadh 11159, Saudi Arabia
[7]Department of Medical Genetics, King Faisal Specialist Hospital and Research Center, Riyadh 11211, Saudi Arabia
[8]Department of Pediatrics, King Fahad General Hospital, Jeddah 23325, Saudi Arabia
[9]Department of Pediatrics, Armed Forces Hospital, Khamis Mushayt 62413, Saudi Arabia
[10]Department of Obstetrics & Gynecology, King Faisal Specialist Hospital, Riyadh 11211, Saudi Arabia
[11]Center of Excellence for Genomics, King Abdulaziz City for Science and Technology, Riyadh 11442, Saudi Arabia
[12]Department of Pediatrics, Security Forces Hospital, Riyadh 12625, Saudi Arabia
[13]Department of Neurosciences, King Faisal Specialist Hospital and Research Center, Riyadh 11211, Saudi Arabia
[14]Division of Genetics, Department of Pediatrics, King Saud bin Abdulaziz University for Health Sciences, King Abdulaziz Medical City, Riyadh 14611, Saudi Arabia
[15]Department of Obstetrics and Gynecology, College of Medicine, King Saud University, Riyadh 11451, Saudi Arabia
[16]Department of Psychiatry, College of Medicine, King Saud University, Riyadh 11451, Saudi Arabia
[17]Department of Clinical Genetics, Human Genetics and Genome Research Division, National Research Centre, Cairo 12345, Egypt
[18]Department of Pediatrics, Johns Hopkins Aramco Healthcare, Dhahran 34465, Saudi Arabia
[19]Department of Pediatrics, Children's Hospital, Ain Shams University, Cairo 01234, Egypt
[20]Department of Molecular Biophysics and Biochemistry, Yale University, New Haven, CT 06520, USA
[21]Saudi Human Genome Program, King Abdulaziz City for Science and Technology, Riyadh 11442, Saudi Arabia
[22]Department of Internal Medicine, College of Medicine, King Saud University, Riyadh 11451, Saudi Arabia
[23]Co-first author
*Correspondence: falkuraya@kfshrc.edu.sa
http://dx.doi.org/10.1016/j.celrep.2014.12.015

SUMMARY

Our knowledge of disease genes in neurological disorders is incomplete. With the aim of closing this gap, we performed whole-exome sequencing on 143 multiplex consanguineous families in whom known disease genes had been excluded by autozygosity mapping and candidate gene analysis. This prescreening step led to the identification of 69 recessive genes not previously associated with disease, of which 33 are here described (*SPDL1*, *TUBA3E*, *INO80*, *NID1*, *TSEN15*, *DMBX1*, *CLHC1*, *C12orf4*, *WDR93*, *ST7*, *MATN4*, *SEC24D*, *PCDHB4*, *PTPN23*, *TAF6*, *TBCK*, *FAM177A1*, *KIAA1109*, *MTSS1L*, *XIRP1*, *KCTD3*, *CHAF1B*, *ARV1*, *ISCA2*, *PTRH2*, *GEMIN4*, *MYOCD*, *PDPR*, *DPH1*, *NUP107*, *TMEM92*, *EPB41L4A*, and *FAM120AOS*). We also encountered instances in which the phenotype departed significantly from the established clinical presentation of a known disease gene. Overall, a likely causal mutation was identified in >73% of our cases. This study contributes to the global effort toward a full compendium of disease genes affecting brain function.

INTRODUCTION

Neurogenetic disorders represent the largest category of Mendelian diseases in humans. They encompass a wide array of

clinical presentations that range from the common e.g., intellectual disability (>1%) to the very rare, e.g., neurodegeneration with brain iron accumulation (one to three per 10^6) (Kalman et al., 2012; Maulik et al., 2011). The highly prevalent involvement of the nervous system in many Mendelian disorders coincides with the observation that >80% of all human genes are expressed at some stage of brain development (Hawrylycz et al., 2012) and suggests that the brain is one of the most vulnerable organs to genetic perturbation. In fact high-resolution microarray analysis of the human genome reveals that intellectual disability is the common phenotypic denominator of genomic disorders that involve losses or gains of genes (Coe et al., 2012).

Variances in clinical presentation are a major obstacle in establishing a working molecular classification of neurological disease, because even where the clinical presentation is highly specific, genetic heterogeneity is the rule. In the setting of autosomal recessive neurogenetic disorders where parents are related, a homozygosity scan can serve as a guide to the underlying genetic cause even when the phenotype is atypical (Alkuraya, 2010). Another major challenge in assigning a molecular classification is that many neurological disease genes have not been identified yet.

Novel disease gene discovery in this field has been tremendously abetted by next-generation sequencing, a tool with the capacity to, theoretically, unravel the genetic cause of all neurological diseases. This full theoretical potential has not yet been reached unfortunately, although the technology continues to evolve. For example, two large studies on the genetics of intellectual disability using whole-exome sequencing (WES) provided a yield of 16%–55%, and even though the collective sample size was >150, only seven novel genes were identified (de Ligt et al., 2012; Rauch et al., 2012). In these studies, samples could not be enriched for novel gene discovery, and simultaneously the anticipated mutations were heterozygous, detection of which poses a challenge for the currently available sequencing technology (especially regarding insertions/deletions) (Harismendy et al., 2009). The presence of these two obstacles likely hindered the authors' ability to obtain a higher yield. Thus, alternative/complementary approaches are required to facilitate the discovery of novel neurogenetic disease genes. In this study, we show that the analysis of the entire set of autozygous intervals per individual (the autozygome) in multiplex consanguineous patients, as a prescreen, can markedly increase the yield of WES to identify candidate genes not previously associated with disease. Even when known genes were identified using this approach, the phenotype was often sufficiently different to explain why the gene had been missed by the autozygosity filter. The 33 candidate disease genes we showcase in this study will augment the global hunt for the genetics of brain development and function.

RESULTS

Clinical Report

In total, 143 multiplex families met our inclusion criteria (a neurogenetic diagnosis, positive family history, consanguineous parents, and no candidates identified by autozygosity mapping). Intellectual disability was the most common clinical feature. Other phenotypes that were also enriched included global developmental delay, autism, epilepsy, primary microcephaly, ataxia, and neurodegeneration. Table S1 summarizes the clinical features of the entire cohort.

Autozygosity Mapping Is a Powerful Enrichment Tool for Novel Candidate Gene Discovery

As a prescreening step for each case, the regions of homozygosity (ROH), the telltale sign of shared ancestral haplotypes, were interrogated for disease genes that matched the patients' phenotype. These genes were prioritized for Sanger sequencing. If negative, or when no compelling disease genes were evident in the ROH, patient DNA was subjected to WES under the assumption that this will reveal a novel disease gene. This assumption fails, however, to account for certain scenarios. When disease genes within the ROH are examined for a likely candidate, it is possible that the clinical picture may sufficiently deviate from the classical phenotype ascribed to a particular gene such that the gene falls outside our consideration. Specifically, we list in Table 1 cases in which there was sufficient discrepancy between the classical and observed phenotypes that the respective genes were missed in the autozygosity mapping stage. Some phenotypes can even be considered unique rather than an expansion of a known phenotype.

A second reason why WES may reveal a known disease gene is that the causal mutation may lie within an ROH but fail to be detected, which is one of the known "pitfalls" of autozygosity mapping (Alkuraya, 2012). Figure S1 captures the homozygosity pattern of a number of patients for whom the candidate ROH was missed, because it did not meet our ROH size cutoff, or it appeared to be shared by an unaffected member of the family, or the overlap of the gene with the ROH was not clearly discernible. One case (11DG0165) evaded detection due to the presence of a deep intronic mutation, which was later uncovered using RT-PCR. A third scenario for why WES may expose a known disease gene is that the gene was simply overlooked when searching for plausible candidates within an ROH. This occurred in 13DG1803 where *TUSC3*, a known intellectual disability gene, was not noticed during the prescreening stage. Further scenarios include incomplete clinical information at the time of analysis (as occurred with 09DG-00774 and 12DG0926) and poor description in the literature (discussed below). We emphasize, however, that cases of failed autozygosity map prescreening are the exception rather than the rule because they represent only ~7.7% (11/143) of all cases and have reduced the hypothetical yield of WES in revealing candidate genes not associated with disease, or known genes with unique phenotypes, by only 2.2%.

WES Is a Powerful Novel Candidate Gene Discovery Tool in Neurogenetic Disorders

Consistent with our prescreening enrichment step, WES revealed 69 genes that were not known to the authors at the time of exome capture. Of these, 36 have since been published by either us or others (detailed in Table S1), leaving 33 candidate genes that are here reported. The phenotypes associated with these are described in Table 2 and include intellectual disability, autism, progressive cerebellar atrophy, primary microcephaly, brain atrophy and other malformations, and myopathy. Of these

Table 1. Cases with Mutations in Known Disease Genes following WES, Where the Patient Phenotype Diverged from the Established Literature

ID	Gene	Mutation	Published Phenotype	Observed Phenotype	Reference
09DG0057	*GM2A*	NM_000405.4:c.164C > T:p.P55L	GM2-gangliosidosis, AB variant	progressive neurodegeneration with onset at 8 years, no organomegaly and normal retina	this study
12DG0096	*SPG20*	NM_001142294:c.1450_1451insA:p.T484fs	spastic paraplegia	speech and motor delay, tremor, microcephaly, and strabismus	this study
12DG1571	*CYP27A1*	NM_000784:c.1342C > T:p.R448C	cerebrotendinous xanthomatosis	severe choreoathetosis, no cataract, and normal cholestanol	this study
10DG0672	*NPC2*	NM_006432:c.88G > A: p.V30M	Nieman-Pick disease	microcephaly, static encephalopathy, no organomegaly, and normal retina	this study
11DG1951	*ARFGEF2*	NM_006420:c.656_657insC:p.P219fs	periventricular heterotopia with microcephaly	global developmental delay, epilepsy, and hydrocephalus	this study
11DG1510	*PNKP*	NM_007254:c.1250_1251insAACGGGTCGCCATCGAC:p.R418Tfs*55	progressive microcephaly, infantile-onset seizures, and developmental delay	primary microcephaly, global developmental delay, no seizures	this study
12DG0975	*RYR1*	NM_000540:c.6617C > T:p.T2206M	minicore myopathy	ptosis, no motor delay, and sacral agenesis	this study
12DG0104	*FBN2*	NM_001999:c.1064G > A:p.G355D	congenital contractural arachnodactyly	fetal akinesia with brain ischemia and neonatal death	this study
08DG00385	*BRCA2*	NM_000059.3:c.9152 delC:p.P3051Hfs*11	Fanconi anemia	primordial dwarfism	Shaheen et al. (2014)
10DG1721	*EVC2*	NM_147127.4:c.3870_3893 dup:p.K1293_K1300 dup	Ellis-van-Creveld syndrome	Meckel-Gruber syndrome	Shaheen et al. (2013)
13DG0583	*DDHD2*	NM_015214.2:c.1249_1891 del:p.A417Mfs*23 (large scale deletion)	spastic paraplegia	isolated cerebellar atrophy	this study
13DG0010	*WDR81*	NM_001163809:c.845G > A:p.G282E	cerebellar ataxia, mental retardation, and dysequilibrium syndrome-2	neonatal death due to severe brain malformation (hydranencephaly and severe cerebellar hypoplasia)	this study
12DG0685	*ZNF526*	NM_133444:c.479A > C:p.K160T	nonsyndromic intellectual disability	intellectual disability, Noonan-like facies, and pulmonary stenosis	this study
09DG00930	*ADCK3*	NM_020247:c.1744 dup:p.S582Kfs*148	cerebellar ataxia, seizure and cerebellar atrophy	isolated cerebellar hypoplasia	this study
09DG0301	*SBF1*	NM_002972:c.1327G > A:p.D443N	Charcot-Marie-Tooth disease type 4B3	Charcot-Marie-Tooth with microcephaly, ophthalmoplegia and syndactyly	Alazami et al. (2014)
11DG1767	*AP4M1*	NM_004722:c.C952T:p.R318*	spastic paraplegia, severe ID, poor speech development	microcephaly, speech delay, spasticity; brain MRI: hypomyelination, hypoplastic corpus callosum, and brain atrophy.	this study

mutations, ten are truncating or located at splice sites. For the missense changes, we determined pathogenicity based on the in silico prediction of at least two established algorithms, as well as 3D modeling of wild-type and mutant residues whenever structure information on homologous proteins was available (Figure S2). Our minimum threshold for assigning candidacy to a gene was that the variant had to be the only one to survive the stringent pipeline illustrated in Figure 2. A total of 37 cases remain "unsolved," some because more than one variant survived our filters. Table S1 lists these, and it is important to note that some of these variants may indeed represent bona fide novel disease genes.

In addition, WES revealed what appears to be phenotypes that have not been described for the respective genes in 16 cases (Table 1). One striking example is case 10DG0672 in which we identified a previously reported homozygous mutation in *NPC2*, a known gene for Nieman-Pick disease. Neither the index nor his sibling had the typical presentation of progressive neurodegeneration or hepatosplenomegaly, thus making the diagnosis of Nieman-Pick nearly impossible on clinical grounds. Finally, WES also revealed mutations in known genes for cases with classical phenotypes, where the gene was missed either due to a pitfall in autozygosity mapping or incomplete phenotyping (nine cases, discussed above) or because the phenotype was not well described in the literature as in two instances. The first such instance is *MGAT2*-related dysmorphism, which had only been documented by a single photograph (Cormier-Daire et al., 2000). The second instance involves *CTSD*, which was described as causing congenital neuronal ceroid lipofuscinosis when, in fact, the detailed description of the case was severe microlissencephaly and hyperekplexia, which is identical to the phenotype of our case 09DG00288 (Fritchie et al., 2009). Overall, the yield of WES in our cohort was 105 out of 143 (73.4%).

Although we used autozygosity mapping coupled with WES, an alternative strategy is to simply use the mapping information provided by WES analysis. Although most autozygous regions can indeed be inferred by this second strategy, we had previously shown that the use of high-throughput genotyping results in cleaner ROH data with sharper overall resolution (Carr et al., 2013).

3D Modeling of Missense Variants to Support Pathogenicity

3D modeling was performed for selected gene products using the web-based homology modeling engine Phyre2 (Kelley and Sternberg, 2009). Four of the models were built with very high confidence and suggested a pathogenic nature for the identified mutations. In the case of TUBA3E, the model was built based on the structure of tubulin alpha-3E (PDB ID: 3EDL)(Tan et al., 2008) that shares 97% sequence identity with the *TUBA3E* gene product (Figure S2A). The R215C mutation changes the charge distribution on the surface of the protein. Although not participating in microtubule formation (Tan et al., 2008), this site might be involved in the binding of microtubule to other proteins or cofactors. The structure of the gene product of *TSEN15*, human tRNA splicing endonuclease, has been solved by nuclear magnetic resonance (Song and Markley, 2007) (PDB ID: 2GW6). The conserved W76 is embedded inside the protein and is critical in protein folding (Figure S2B). Mutation of W76G would leave a void in the core of the protein and very likely lead to misfolded proteins. *PTRH2* encodes peptidyl-tRNA hydrolase 2. The crystal structure of a domain of PTRH2 has been solved (PDB ID: 1QSR). The observed mutation at Q85 is located in the middle of a helix and forms a hydrogen bond with the side chain of T157 (Figure S2C). Mutation of Q85P would destabilize PTRH2 as it would disrupt the hydrogen bond. Furthermore, the mutation to a proline may cause a kink in the helix and distort the overall fold of the structure. Iron-sulfur cluster assembly 2, or ISCA2, was also modeled with the structure of its homolog of IscA from Thermosynechococcus elongates (PDB ID: 1X0G), which is a $\alpha 2\beta 2$ heterotetramer. ISCA2 has modest sequence identity (27% to PDB ID: 1X0G) to the α chain of the IscA. However, Phyre2 predicted the same structural fold with 100% confidence. The protein is involved in the maturation of iron-sulfur proteins. According to the model, the G77S mutation occurs in a loop that is directly involved in iron-sulfur cluster binding by providing a chelating cysteine, C79 (Figure S2D). We speculate that such a mutation might affect the stability or flexibility of the loop and therefore interfere with its efficiency of binding to the iron-sulfur cluster.

DISCUSSION

Several attempts have been made in the recent past to accelerate the discovery of novel neurological disease genes. One of the earliest attempts was the high-throughput Sanger sequencing of all coding exons on the X chromosome in a large cohort of >200 families with suspected X-linked intellectual disability (Tarpey et al., 2009). In addition to the laborious nature of this approach, the yield was somewhat modest (three novel genes) partly because enrichment for novel gene discovery was not feasible, and also partly due to a large proportion of X-linked disease genes having already been established (de Brouwer et al., 2007). High-resolution molecular karyotyping is a powerful tool to identify a large number of DNA gains and losses that are associated with various neurological phenotypes, but the yield is typically <15%, and it rarely identifies single genes due to the nature of the assay (Miller et al., 2010). Morrow et al. used autozygosity mapping in nearly 90 consanguineous families with autism, followed by Sanger sequencing of candidate genes within the linked ROH, to identify five novel autism genes (Morrow et al., 2008). The lower yield of that study likely originates from the use of conventional sequencing methods, coupled with the potentially non-Mendelian behavior of autism genes.

The advent of next-generation sequencing has revolutionized the search for Mendelian neurocognitive genes. Rauch et al. and de Ligt et al. studied >150 cases of intellectual disability using a trio-exome design, and, although that approach is compatible with identifying recessive disease genes, they only identified heterozygous de novo mutations, including seven novel genes (de Ligt et al., 2012; Rauch et al., 2012). The known bias of current WES against heterozygous mutations, especially insertions and deletions, as well as the inability of the investigators to enrich their cohort for novel genes are likely explanations for the lower

Table 2. Cases with Mutations in Candidate Genes, along with Available Evidence from the Literature to Support Candidacy

ID	Phenotype	Gene	Mutation	Mutation Type	Gene Description	Supporting Evidence	Reference
12DG1528	primary microcephaly and neonatal death	*CCDC99 (SPDL1)*	NM_017785:c.1724_1747 del:p.S575_T582 del	in-frame deletion	spindle apparatus coiled-coil protein 1	CCDC99 has been demonstrated to control poleward movement of chromosomes along the mitotic spindles. Many primary microcephaly genes encode proteins that are involved in mitotic spindle regulation, e.g., ASPM and WDR62. Only surviving variant and segregates in family.	PMID: 20427577 and 24875059
11DG0443	microlissencephaly and global developmental delay	*TUBA3E*	NM_207312:c.643C > T:p.R215C	missense	tubulin, alpha 3e	Mutations in several tubulins have been linked to lissencephaly and other cortical malformations (TUBA1 A, TUBA8, TUBB2B, TUBB3, TUBB5, and TUBG1). Only surviving variant and segregates in family.	PMID: 24860126
10DG1705	primary microcephaly and global developmental delay	*INO80*	INO80:NM_017553: c.1501T > C:p.S501P, INO80:NM_017553: c.3737G > A:p.R1246Q	missense	INO80 complex subunit E	INO80 has been shown as necessary for DNA damage repair. Abnormal DNA damage repair underlies multiple forms of microcephaly, e.g., PHC1 and PNKP. Supported by a single linkage peak. Only surviving variant and segregates in family.	PMID: 21947284, 19829069, 24029917, and 20118933
08DG00041	hydrocephalus, muscle weakness and global developmental delay	*NID1*	NM_002508.2: c.3385+1G > A	splicing (in-frame insertion confirmed by RT-PCR)	Nidogen 1	Mice deficient of NID1 exhibit neurologic deficits including seizure-like symptoms and loss of muscle control in the hind legs and show altered basement membrane morphology in selected locations including brain capillaries and the lens capsule. Additionally, a variant of unknown significance has been reported in a family with brain malformations. Only surviving variant and segregates in family.	PMID: 12480912 and 23674478
13DG0167	primary microcephaly and global developmental delay	*TSEN15*	NM_001127394: c.226T > G:p.W76G	missense	tRNA splicing endonuclease 15	Mutations in other family members, e.g., TSEN54, have been linked to pontocerebellar hypoplasia. Only surviving variant and segregates in family.	PMID: 18711368

(*Continued on next page*)

Table 2. ***Continued***

ID	Phenotype	Gene	Mutation	Mutation Type	Gene Description	Supporting Evidence	Reference
12DG0929	global developmental delay, epilepsy and poor weight gain	*DMBX1*	NM_147192:c.367C > T:p.R123W	missense	diencephalon/ mesencephalon homeobox 1	Mouse model displays hyperactivity and hypophagia. Gene is highly expressed in developing brain. Only surviving variant and segregates in family.	PMID: 15314164 and 17873059
09DG0405	myopathy	*C2orf63 (CLHC1)*	NM_001135598: c.779G > A:p.R260Q	missense	clathrin heavy-chain linker domain containing 1	Mutation in BICD2 which interacts with CLHC1 causes spinal muscular atrophy. Only surviving variant and segregates in family.	PMID: 23664116
09DG00102	global developmental delay	*C12orf4*	NM_020374:exon6: c.637_638insAAAC: p.K213fs	frameshift	chromosome 12 open reading frame 4	Only surviving variant and segregates in family.	
11DG1513	autism spectrum disorder	*WDR93*	NM_020212:c.280T > C:p.Y94H	missense	WD repeat domain 93	Only surviving variant and segregates in family.	
11DG2479	global developmental delay and brain atrophy	*ST7*	NM_021908:c.489T > G:p.Y163X	stopgain	suppression of tumorigenicity 7	Disruption of ST7 has been reported in one ASD patient with a translocation (t(7;13)(q31.3;q21)). Only surviving variant and segregates in family.	PMID: 10889047
12DG1901	holoprosencephaly	*MATN4*	NM_030590:c.515G > C:p.G172A	missense	Matrilin 4	Gene is highly expressed in developing brain. Only surviving variant and segregates in family.	PMID: 11549321
12DG2051	intellectual disability and epilepsy	*SEC24D*	NM_014822:c.697G > C:p.G233R	missense	SEC24 family, member D (*S. cerevisiae*)	Mouse model displays early embryonic lethality, but the mouse model of its paralog SEC24B displays abnormal neural tube development. Only surviving variant and segregates in family.	PMID: 23596517
10DG1069	primary microcephaly and global developmental delay	*PCDHB4*	NM_018938.2:c.915 del:p.K305Nfs*12	frameshift	protocadherin beta 4	PDCHB4 has been associated with autism. Other protocadherin members have been linked to epilepsy, cognitive impairment as well as autistic features. Only surviving variant and segregates in family.	PMID: 22495309 and 22765916
08DG-00322	brain atrophy and global developmental delay	*PTPN23*	NM_015466:c.3995G > T:p.R1332L	missense	protein tyrosine phosphatase, nonreceptor type 23	Mouse model displays early embryonic lethality. Gene is highly expressed in developing brain. Only surviving variant and segregates in family.	PMID: 19378249

(*Continued on next page*)

Table 2. *Continued*

ID	Phenotype	Gene	Mutation	Mutation Type	Gene Description	Supporting Evidence	Reference
11DG0932	global developmental delay and dysmorphism	*TAF6*	NM_005641.3:c.212T > C:p.I71T	missense	TAF6 RNA polymerase II, TATA box binding protein (TBP)-associated factor	Independently identified by another group (B. Yuan, D. Pehlivan, E. Karaca, N.P., W.-L. Charng, T. Gambin, C. Gonzaga-Jauregui, V.R. Sutton, G. Yesil, S.T. Bozdogan, T. Tos, A. Koparir, E. Koparir, C.R. Beck, S. Gu, H. Aslan, O.O. Yuregir, K. Al Rubeaan, D. Alnaqeb, M.J.A., Y. Bayram, M.M. Atik, H. Aydin, B. Geckinli, M. Seven, H. Ulucan, E. Fenercioglu, M. Ozen, S. Jhangiani, D.M. Muzny, E. Boerwinkle, Baylor-Hopkins Center for Mendelian Genomics, B. Tuysuz, F.S.A., R.A. Gibbs, and J.R. Lupski, unpublished data). Only surviving variant and segregates in family.	
10DG1670	global developmental delay, epilepsy, dysmorphism, hypotonia, and VSD	*TBCK*	NM_033115: c.1708+1G > A	splicing (frameshift)	TBC1 domain containing kinase	TBCK knockdown significantly suppresses mTOR signaling, which plays a critical role in multiple neurological disorders. Only surviving variant and segregates in family.	PMID: 23977024, 19963289
13DG1472	macrocephaly, ID, dolichocephaly, and mild obesity	*FAM177A1*	NM_001079519:c.297_298insA:p.L99fs	frameshift	family with sequence similarity 177, member A1	Only surviving variant and segregates in family.	
13DG1900	Dandy-Walker malformation, hydrocephalus, flexed deformity, club feet, micrognathia, and pleural effusion	*KIAA1109*	NM_015312.3:c.1557T > A:p.Y519*	stopgain	KIAA1109	Deletion in Drosophila results in lethality, and the rare homozygous flies that reach adulthood exhibit severe neurological signs: seizures and inability to walk or stand for prolonged period. Only surviving variant and segregates in family.	PMID: 19640479
10DG0264	neurodegeneration and brain iron accumulation	*MTSS1L*	NM_138383:c.1790C > T:p.T597M	missense	metastasis suppressor 1-like	This mutation affects a poorly characterized isoform of *VAC14* deficiency of which in mouse results in severe neurodegeneration. Only surviving variant and segregates in family.	PMID: 17956977

(*Continued on next page*)

Table 2. ***Continued***

ID	Phenotype	Gene	Mutation	Mutation Type	Gene Description	Supporting Evidence	Reference
13DG1935	primary microcephaly	*XIRP1*	NM_194293:c.4495G > A:p.E1499K	missense	xin actin-binding repeat containing 1	Gene is highly expressed in the brain in response to oxidative stress. Only surviving variant and segregates in family.	PMID: 22366181
13DG2274	severe psychomotor retardation, seizure, and cerebellar hypoplasia	*KCTD3*	NM_016121:c.1036_1073 del:p.P346Tfs*4	frameshift	potassium channel tetramerization domain containing 3	Gene is enriched in copy number changes associated with intellectual disability. Supported by a single linkage peak. Only surviving variant and segregates in family.	PMID: 19623214
13DG0832	global developmental delay and ADHD	*CHAF1B*	NM_005441:c.496A > G:p.I166V	missense	chromatin assembly factor 1, subunit B	CHAF1B is part of the chromatin assembly complex deficiency of which results in loss of asymmetry during nervous system development in *C. elegans*. Only surviving variant and segregates in family.	PMID: 22177093
08DGRC00077	neurodegenerative disease	*ARV1*	NM_022786:c.565G > A:p.G189R	missense	ARV1 homolog (*S. cerevisiae*)	ARV1 is required for normal sphingolipid metabolism, a process known to be defective in other neurodegenerative diseases such as Nieman-Pick disease. Only surviving variant and segregates in family.	PMID: 12145310
14DG0152	neurodegeneration with marked white matter changes with high lactate peak in the brain, consistent with mitochondrial encephalopathy	*ISCA2*	NM_194279:c.229G > A:p.G77S	missense	iron-sulfur cluster assembly 2 homolog	Maps to the only shared haplotype in the extended family. ISCA2 is a member of mitochondrial iron-sulfur cluster (ISC) assembly machinery. Depletion of ISCA2 results in massively swollen mitochondria that are devoid of cristae membranes indicating that it is required for normal mitochondrial biogenesis. Same mutation was identified in other families with identical presentation (Z.N.A.-H., M. Al-Dosary, M. Alfadhel, E.F., M. Alsagob, R. Kenana, R. Almas, O.S. Al-Harazi, H. Al-Hindi, O.I. Malibari, F.B. Almutari, T. Al-Sheddi, S. Tulbah, F. Alhadeq, R. Alamro, A, AlAsmari, M. Almuntashri, H. Alshaalan, F.A. Al-Mohanna, D. Colak, N.K., unpublished data). Only surviving variant and segregates in family.	PMID: 22323289

(*Continued on next page*)

Table 2. *Continued*

ID	Phenotype	Gene	Mutation	Mutation Type	Gene Description	Supporting Evidence	Reference
13DG0215	global developmental delay, hearing loss, and ataxia	*PTRH2*	NM_016077.3:c.254A > C:p.Q85P	missense	peptidyl-tRNA hydrolase 2	Null mice show ataxia and weakness; tissue examination revealed delayed development. Only surviving variant and segregates in family.	PMID: 18218778
08DG0048510DG070313DG1542	(08DG00485) global developmental delay, severe dystonia, and congenital cataract (10DG0703) global developmental delay and congenital cataract(13DG1542) global developmental delay, congenital cataract, tubulopathy, and severe osteopenia	*GEMIN4*	NM_015721:c.2452T > C:p.W818R	missense	gem (nuclear organelle) associated protein 4	Maps to the only shared haplotype in the three families. GEMIN4 is part of the SMN complex, and reduced SMN protein results in spinal muscular atrophy. Supported by a single linkage peak. Only surviving variant and segregates in family.	PMID: 11914277
13DG1549	intellectual disability and epilepsy	*MYOCD*	NM_001146312: c.1252A > G:p.I418V	missense	myocardin	Only surviving variant and segregates in family.	PMID: 12867591
13DG0274	global developmental delay, typical Joubert syndrome, MRI findings	*PDPR*	NM_017990:c.1360G > T:p.G454C	missense	pyruvate dehydrogenase phosphatase regulatory subunit	Only surviving variant and segregates in family.	
10DG0934	cerebellar vermis hypoplasia, Dandy-Walker malformation, hydrocephalus, developmental delay	*DPH1*	NM_001383.3:c.701T > C:p.L234P	missense	diphthamide biosynthesis 1	Diphthamide is a unique posttranslationally modified histidine found only in translation elongation factor-2 (eEF2), which is linked to spinocerebellar ataxia. Diphthamide modification of eEF2 is essential for normal mouse development. Only surviving variant and segregates in family.	PMID: 18765564
11DG0417	global developmental delay, light complexion, early onset focal segmental glomerulosclerosis	*NUP107*	NM_020401:c.303G > A:p.M101I	splice site	nucleoporin 107 kDa	Only surviving variant and segregates in family.	
14DG0221	cerebellar atrophy, hydrocephalus, and global developmental (cognitive, speech, and motor) delay	*TMEM92*	NM_001168215: c.95+3A > G	splice site	transmembrane protein 92	Only surviving variant and segregates in family.	

(*Continued on next page*)

Table 2. *Continued*

ID	Phenotype	Gene	Mutation	Mutation Type	Gene Description	Supporting Evidence	Reference
10DG0840	spastic paraplegia, failure to thrive.	*EPB41L4A*	NM_022140:c.1298C > T:p.S433L	missense	erythrocyte membrane protein band 4.1 like 4A	Only surviving variant and segregates in family.	
12DG0321	coarse facial features (open mouth, bilateral ptosis, and hypertelorism), scoliosis, pectus excavatum, skin laxity, hypotonia, GERD, chronic lung disease, undescended testicles.	*FAM120AOS*	NM_198841:c.743C > T:p.T248I	missense	family with sequence similarity 120A opposite strand	Only surviving variant and segregates in family.	

yield. In 2011, Najmabadi et al. reported the identification of 50 novel candidate genes (Najmabadi et al., 2011). Although that study, similar to ours, combines autozygosity mapping with next-generation sequencing of candidate ROH, their cohort was not enriched for novel gene discovery. Consequently, there were numerous cases that, upon exome sequencing, identified a gene that was classically linked to the clinical presentation (as per their Table 1). More importantly, the pipeline used in that study did not strictly require that the candidate variant be the only one to survive filtering in that family; hence, 24 of their candidate genes (48%) were not the sole surviving variant. Of the remainder, one variant (*HIST3H3*) is present at sufficiently high frequency in our collection of 485 exomes to be excluded (allele frequency 0.0082).

Beyond our analytic pipeline, the candidacy of many of our candidate genes can be corroborated through other lines of evidence. In the case of *INO80*, *KCTD3*, *GEMIN4*, and *ISCA2*, each of these genes maps to the only shared haplotype genome-wide across multiple or extended multiplex families (Figure S3). TUBA3E belongs to a family of proteins that are known to be involved in brain malformation syndromes including lissencephaly, which is present in the affected patient (Figure S4) (Jaglin et al., 2009; Keays et al., 2007; Poirier et al., 2010). As well, TSEN15 belongs to a family of proteins (t-RNA splicing endonucleases) that have been found mutated in patients with pontocerebellar hypoplasia and microcephaly, which is what we observed in our patient (Budde et al., 2008; Cassandrini et al., 2010; Namavar et al., 2011). SPDL1 controls poleward movement of chromosomes along the mitotic spindles, analogous to many of the known primary microcephaly genes that are involved in mitotic spindle regulation (Barisic et al., 2010; Chen et al., 2014); our patient exhibits an extreme reduction in overall brain volume resulting in an almost empty skull (Figure S4). ISCA2 is involved in mitochondrial protein maturation, and depletion of the protein results in massively swollen mitochondria that are devoid of cristae membranes (Sheftel et al., 2012). This is consistent with the mitochondrial encephalopathy detected in our patient. Table 2 summarizes what is known of the 33 candidate genes and available evidence that supports candidacy.

We were unable to identify a causal mutation in 25.9% of cases. Many of these have two or more variants that remained after filtering (Table S1), leaving open the possibility that one of these surviving variants may indeed be causal. Some of these are strong candidates. For instance, case 11DG0375 with brain atrophy has the first reported null mutation in *SNCG*, which encodes synuclein-γ, and, although a role in neurodegeneration has been suspected, such a role has remained elusive (Greten-Harrison et al., 2010). Similarly, TRIM4 is a member of a family of proteins that has been implicated in a number of neurological disorders (TRIM2 in Charcot-Marie-Tooth, TRIM32 in Limb-Girdle Muscular Dystrophy, and TRIM18 in Opitz-GBBB (a syndromic form of intellectual disability) (Balastik et al., 2008; Frosk et al., 2002; Quaderi et al., 1997). Thus, the homozygous *TRIM4* truncation we identified in 12DG2083 may prove causal if additional mutations in this gene are identified in the future.

Cases in which no variants survived our filters may harbor classes of mutations that either the sequencing technology or our analysis pipeline are biased against e.g., compound

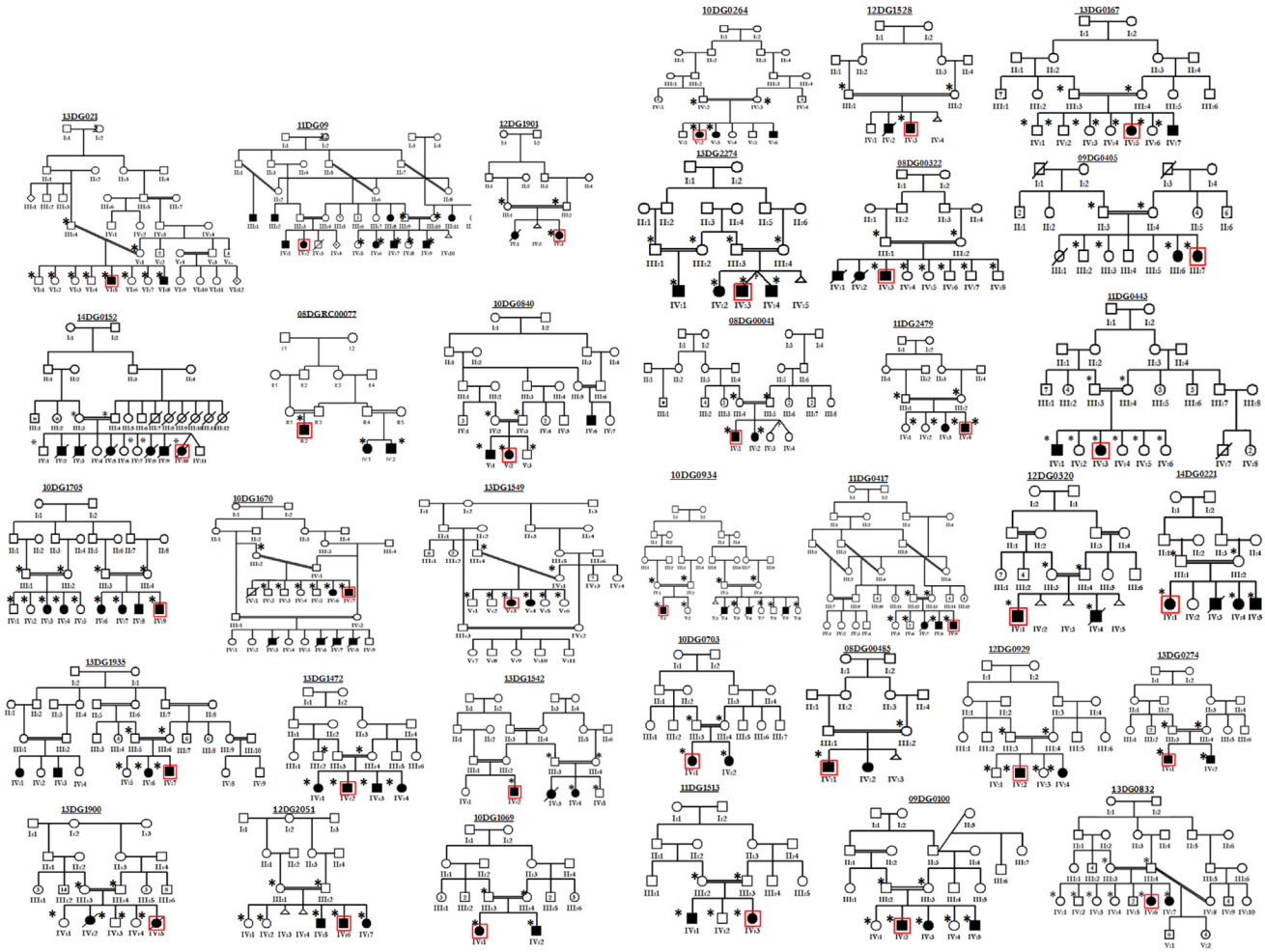

Figure 1. Pedigrees of Families with Novel Candidate Genes following WES Analysis

The family ID is presented above each pedigree. A red box indicates the affected family member who was submitted for WES, and asterisks denote all the family members we had access to for confirming segregation.

heterozygous mutations, X-linked mutations, or mutations involving introns, UTRs, regulatory elements, and repeats. Nonetheless, our study clearly shows the utility of our approach when applied in the right population. Our pipeline as mentioned here has been very successful historically. Many unpublished genes we highlighted as novel and disease causing at the time of data analysis were subsequently published and verified by others, and this lends weight to the candidacy of the genes we report here. Indeed, such reports appeared as recently as a few months from this submission, e.g., *DIAPH1*, *PIGQ*, and *WWOX* (Ercan-Sencicek et al., 2014; Mallaret et al., 2014; Martin et al., 2014). This is also true for certain variants in "unsolved" cases where more than one variant remained, e.g., *SLC13A5* (Thevenon et al., 2014). Our aim in publishing these 33 candidate genes is to accelerate the discovery of other independent mutations, thereby confirming pathogenicity and assisting in genetic diagnosis. Scaling of our study is feasible given the availability of the appropriate patient samples and the dropping cost of sequencing technology, with the promise that all autosomal recessive neurogenetic disease genes can be mapped within the timeframe required by the global brain initiatives.

EXPERIMENTAL PROCEDURES

Human Subjects

Consanguineous families with history of a neurological disorder were clinically evaluated and recruited for this study using a King Faisal Specialist Hospital and Research Center institutional-review-board-approved protocol (RAC# 2121053) with informed consent. All families were multiplex, and all parents were confirmed to be healthy. Pedigrees of families with the 33 candidate genes are given in Figure 1. For each family, blood was collected in EDTA tubes from all available members, and families were only included if at least one affected individual was available for sampling. DNA was extracted from whole blood using standard protocols.

Autozygome-Guided Mutation Analysis

Genome-wide SNP genotyping and homozygosity mapping was performed using the AxiomGWH SNP Chip platform (Affymetrix). See Supplemental Information for more details. Genes known to cause a neurological disorder compatible with the patients' phenotype, and present within the autozygome,

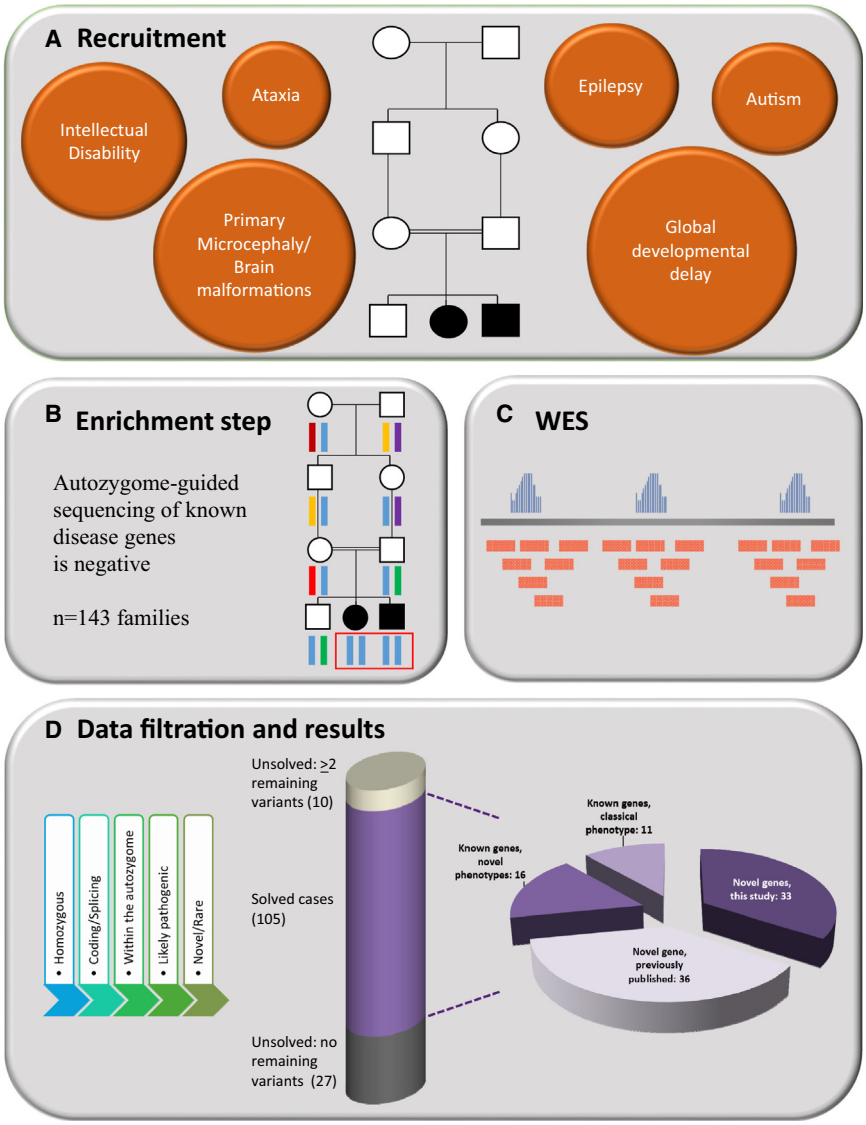

Figure 2. Schematic of the Experimental Pipeline for This Study

A total of 143 multiplex consanguineous families with history of a neurological disorder were found negative for known disease genes following autozygome-guided analysis and were recruited for this study. The bar illustrates the breakdown based on the number of cases, whereas the pie chart is based on the number of distinct genes identified in the solved cases.

were screened by PCR and Sanger sequencing. If no such genes existed, or if they did exist but were excluded by sequencing, exome capture was performed. In total, individuals from 143 families were exome sequenced, and these families formed the cohort for this study.

Exome Sequencing

Exome capture was performed using the TruSeq Exome Enrichment kit (Illumina). See Supplemental Information for more details. A summary of the quality control data for exome sequencing is provided in Table S2.

Analysis of Exomic Variants

Exome-derived data were filtered according to the schematic in Figure 2. See Supplemental Information for full details. Segregation was assessed for all surviving variants, using all family members we had access to (Figure 1).

ACCESSION NUMBERS

All variants within the 143 exomes in this study can be accessed through the following link (part of the Saudi Variome Database): http://shgp.kfshrc.edu.sa/bioinf/db/variants/dg/index.html. The ClinVar accession numbers for the novel variants in this paper are SCV000196382–SCV000196477.

SUPPLEMENTAL INFORMATION

Supplemental Information includes two figures and two tables and can be found with this article online at http://dx.doi.org/10.1016/j.celrep.2014.12.015.

AUTHOR CONTRIBUTIONS

A.M.A. collected and analyzed data and wrote the manuscript, N.P. collected and analyzed data and wrote the manuscript, H.E.S. collected and analyzed data and wrote the manuscript.

ACKNOWLEDGMENTS

We thank all the families for their enthusiastic participation. This work was funded in part by KACST 13-BIO1113-20 (F.S.A.). We acknowledge the Saudi Human Genome Project for infrastructure and informatics support relating to

work presented in this manuscript. We are also grateful to the sequencing core facility, and to Salma Wakil and the genotyping core facility, at KFSH&RC for their invaluable assistance. M.A.S. was supported by the Deanship of Scientific Research, King Saud University, Riyadh, Saudi Arabia through Research Group no. RGP-VPP-301.

Received: August 21, 2014
Revised: November 19, 2014
Accepted: December 8, 2014
Published: December 31, 2014

REFERENCES

Alazami, A.M., Alzahrani, F., Bohlega, S., and Alkuraya, F.S. (2014). SET binding factor 1 (SBF1) mutation causes Charcot-Marie-tooth disease type 4B3. Neurology *82*, 1665–1666.

Alkuraya, F.S. (2010). Homozygosity mapping: one more tool in the clinical geneticist's toolbox. Genet. Med. *12*, 236–239.

Alkuraya, F.S. (2012). Discovery of rare homozygous mutations from studies of consanguineous pedigrees. Curr. Protoc. Hum. Genet. *6*, 16.12.

Balastik, M., Ferraguti, F., Pires-da Silva, A., Lee, T.H., Alvarez-Bolado, G., Lu, K.P., and Gruss, P. (2008). Deficiency in ubiquitin ligase TRIM2 causes accumulation of neurofilament light chain and neurodegeneration. Proc. Natl. Acad. Sci. USA *105*, 12016–12021.

Barisic, M., Sohm, B., Mikolcevic, P., Wandke, C., Rauch, V., Ringer, T., Hess, M., Bonn, G., and Geley, S. (2010). Spindly/CCDC99 is required for efficient chromosome congression and mitotic checkpoint regulation. Mol. Biol. Cell *21*, 1968–1981.

Budde, B.S., Namavar, Y., Barth, P.G., Poll-The, B.T., Nürnberg, G., Becker, C., van Ruissen, F., Weterman, M.A., Fluiter, K., te Beek, E.T., et al. (2008). tRNA splicing endonuclease mutations cause pontocerebellar hypoplasia. Nat. Genet. *40*, 1113–1118.

Carr, I.M., Bhaskar, S., O'Sullivan, J., Aldahmesh, M.A., Shamseldin, H.E., Markham, A.F., Bonthron, D.T., Black, G., and Alkuraya, F.S. (2013). Autozygosity mapping with exome sequence data. Hum. Mutat. *34*, 50–56.

Cassandrini, D., Biancheri, R., Tessa, A., Di Rocco, M., Di Capua, M., Bruno, C., Denora, P.S., Sartori, S., Rossi, A., Nozza, P., et al. (2010). Pontocerebellar hypoplasia: clinical, pathologic, and genetic studies. Neurology *75*, 1459–1464.

Chen, J.-F., Zhang, Y., Wilde, J., Hansen, K.C., Lai, F., and Niswander, L. (2014). Microcephaly disease gene Wdr62 regulates mitotic progression of embryonic neural stem cells and brain size. Nat. Commun. *5*, 3885.

Coe, B.P., Girirajan, S., and Eichler, E.E. (2012). A genetic model for neurodevelopmental disease. Curr. Opin. Neurobiol. *22*, 829–836.

Cormier-Daire, V., Amiel, J., Vuillaumier-Barrot, S., Tan, J., Durand, G., Munnich, A., Le Merrer, M., and Seta, N. (2000). Congenital disorders of glycosylation IIa cause growth retardation, mental retardation, and facial dysmorphism. J. Med. Genet. *37*, 875–877.

de Brouwer, A.P., Yntema, H.G., Kleefstra, T., Lugtenberg, D., Oudakker, A.R., de Vries, B.B., van Bokhoven, H., Van Esch, H., Frints, S.G., Froyen, G., et al. (2007). Mutation frequencies of X-linked mental retardation genes in families from the EuroMRX consortium. Hum. Mutat. *28*, 207–208.

de Ligt, J., Willemsen, M.H., van Bon, B.W., Kleefstra, T., Yntema, H.G., Kroes, T., Vulto-van Silfhout, A.T., Koolen, D.A., de Vries, P., Gilissen, C., et al. (2012). Diagnostic exome sequencing in persons with severe intellectual disability. N. Engl. J. Med. *367*, 1921–1929.

Ercan-Sencicek, A.G., Jambi, S., Franjic, D., Nishimura, S., Li, M., El-Fishawy, P., Morgan, T.M., Sanders, S.J., Bilguvar, K., Suri, M., et al. (2014). Homozygous loss of DIAPH1 is a novel cause of microcephaly in humans. Eur. J. Hum. Genet.

Fritchie, K., Siintola, E., Armao, D., Lehesjoki, A.-E., Marino, T., Powell, C., Tennison, M., Booker, J.M., Koch, S., Partanen, S., et al. (2009). Novel mutation and the first prenatal screening of cathepsin D deficiency (CLN10). Acta Neuropathol. *117*, 201–208.

Frosk, P., Weiler, T., Nylen, E., Sudha, T., Greenberg, C.R., Morgan, K., Fujiwara, T.M., and Wrogemann, K. (2002). Limb-girdle muscular dystrophy type 2H associated with mutation in TRIM32, a putative E3-ubiquitin-ligase gene. Am. J. Hum. Genet. *70*, 663–672.

Greten-Harrison, B., Polydoro, M., Morimoto-Tomita, M., Diao, L., Williams, A.M., Nie, E.H., Makani, S., Tian, N., Castillo, P.E., Buchman, V.L., and Chandra, S.S. (2010). αβγ-Synuclein triple knockout mice reveal age-dependent neuronal dysfunction. Proc. Natl. Acad. Sci. USA *107*, 19573–19578.

Harismendy, O., Ng, P.C., Strausberg, R.L., Wang, X., Stockwell, T.B., Beeson, K.Y., Schork, N.J., Murray, S.S., Topol, E.J., Levy, S., and Frazer, K.A. (2009). Evaluation of next generation sequencing platforms for population targeted sequencing studies. Genome Biol. *10*, R32.

Hawrylycz, M.J., Lein, E.S., Guillozet-Bongaarts, A.L., Shen, E.H., Ng, L., Miller, J.A., van de Lagemaat, L.N., Smith, K.A., Ebbert, A., Riley, Z.L., et al. (2012). An anatomically comprehensive atlas of the adult human brain transcriptome. Nature *489*, 391–399.

Jaglin, X.H., Poirier, K., Saillour, Y., Buhler, E., Tian, G., Bahi-Buisson, N., Fallet-Bianco, C., Phan-Dinh-Tuy, F., Kong, X.P., Bomont, P., et al. (2009). Mutations in the β-tubulin gene TUBB2B result in asymmetrical polymicrogyria. Nat. Genet. *41*, 746–752.

Kalman, B., Lautenschlaeger, R., Kohlmayer, F., Büchner, B., Kmiec, T., Klopstock, T., and Kuhn, K.A. (2012). An international registry for neurodegeneration with brain iron accumulation. Orphanet J. Rare Dis. *7*, 66.

Keays, D.A., Tian, G., Poirier, K., Huang, G.-J., Siebold, C., Cleak, J., Oliver, P.L., Fray, M., Harvey, R.J., Molnár, Z., et al. (2007). Mutations in α-tubulin cause abnormal neuronal migration in mice and lissencephaly in humans. Cell *128*, 45–57.

Kelley, L.A., and Sternberg, M.J. (2009). Protein structure prediction on the Web: a case study using the Phyre server. Nat. Protoc. *4*, 363–371.

Mallaret, M., Synofzik, M., Lee, J., Sagum, C.A., Mahajnah, M., Sharkia, R., Drouot, N., Renaud, M., Klein, F.A., and Anheim, M. (2014). The tumour suppressor gene WWOX is mutated in autosomal recessive cerebellar ataxia with epilepsy and mental retardation. Brain *137*, 411–419.

Martin, H.C., Kim, G.E., Pagnamenta, A.T., Murakami, Y., Carvill, G.L., Meyer, E., Copley, R.R., Rimmer, A., Barcia, G., Fleming, M.R., et al.; WGS500 Consortium (2014). Clinical whole-genome sequencing in severe early-onset epilepsy reveals new genes and improves molecular diagnosis. Hum. Mol. Genet. *23*, 3200–3211.

Maulik, P.K., Mascarenhas, M.N., Mathers, C.D., Dua, T., and Saxena, S. (2011). Prevalence of intellectual disability: a meta-analysis of population-based studies. Res. Dev. Disabil. *32*, 419–436.

Miller, D.T., Adam, M.P., Aradhya, S., Biesecker, L.G., Brothman, A.R., Carter, N.P., Church, D.M., Crolla, J.A., Eichler, E.E., Epstein, C.J., et al. (2010). Consensus statement: chromosomal microarray is a first-tier clinical diagnostic test for individuals with developmental disabilities or congenital anomalies. Am. J. Hum. Genet. *86*, 749–764.

Morrow, E.M., Yoo, S.-Y., Flavell, S.W., Kim, T.-K., Lin, Y., Hill, R.S., Mukaddes, N.M., Balkhy, S., Gascon, G., Hashmi, A., et al. (2008). Identifying autism loci and genes by tracing recent shared ancestry. Science *321*, 218–223.

Najmabadi, H., Hu, H., Garshasbi, M., Zemojtel, T., Abedini, S.S., Chen, W., Hosseini, M., Behjati, F., Haas, S., Jamali, P., et al. (2011). Deep sequencing reveals 50 novel genes for recessive cognitive disorders. Nature *478*, 57–63.

Namavar, Y., Barth, P.G., Kasher, P.R., van Ruissen, F., Brockmann, K., Bernert, G., Writzl, K., Ventura, K., Cheng, E.Y., Ferriero, D.M., et al.; PCH Consortium (2011). Clinical, neuroradiological and genetic findings in pontocerebellar hypoplasia. Brain *134*, 143–156.

Poirier, K., Saillour, Y., Bahi-Buisson, N., Jaglin, X.H., Fallet-Bianco, C., Nabbout, R., Castelnau-Ptakhine, L., Roubertie, A., Attie-Bitach, T., Desguerre, I., et al. (2010). Mutations in the neuronal ß-tubulin subunit TUBB3 result in malformation of cortical development and neuronal migration defects. Hum. Mol. Genet. *19*, 4462–4473.

Quaderi, N.A., Schweiger, S., Gaudenz, K., Franco, B., Rugarli, E.I., Berger, W., Feldman, G.J., Volta, M., Andolfi, G., Gilgenkrantz, S., et al. (1997). Opitz

G/BBB syndrome, a defect of midline development, is due to mutations in a new RING finger gene on Xp22. Nat. Genet. *17*, 285–291.

Rauch, A., Wieczorek, D., Graf, E., Wieland, T., Endele, S., Schwarzmayr, T., Albrecht, B., Bartholdi, D., Beygo, J., Di Donato, N., et al. (2012). Range of genetic mutations associated with severe non-syndromic sporadic intellectual disability: an exome sequencing study. Lancet *380*, 1674–1682.

Shaheen, R., Faqeih, E., Alshammari, M.J., Swaid, A., Al-Gazali, L., Mardawi, E., Ansari, S., Sogaty, S., Seidahmed, M.Z., AlMotairi, M.I., et al. (2013). Genomic analysis of Meckel-Gruber syndrome in Arabs reveals marked genetic heterogeneity and novel candidate genes. Eur. J. Hum. Genet. *21*, 762–768.

Shaheen, R., Faqeih, E., Ansari, S., Abdel-Salam, G., Al-Hassnan, Z.N., Al-Shidi, T., Alomar, R., Sogaty, S., and Alkuraya, F.S. (2014). Genomic analysis of primordial dwarfism reveals novel disease genes. Genome Res. *24*, 291–299.

Sheftel, A.D., Wilbrecht, C., Stehling, O., Niggemeyer, B., Elsässer, H.-P., Mühlenhoff, U., and Lill, R. (2012). The human mitochondrial ISCA1, ISCA2, and IBA57 proteins are required for [4Fe-4S] protein maturation. Mol. Biol. Cell *23*, 1157–1166.

Song, J., and Markley, J.L. (2007). Three-dimensional structure determined for a subunit of human tRNA splicing endonuclease (Sen15) reveals a novel dimeric fold. J. Mol. Biol. *366*, 155–164.

Tan, D., Rice, W.J., and Sosa, H. (2008). Structure of the kinesin13-microtubule ring complex. Structure *16*, 1732–1739.

Tarpey, P.S., Smith, R., Pleasance, E., Whibley, A., Edkins, S., Hardy, C., O'Meara, S., Latimer, C., Dicks, E., Menzies, A., et al. (2009). A systematic, large-scale resequencing screen of X-chromosome coding exons in mental retardation. Nat. Genet. *41*, 535–543.

Thevenon, J., Milh, M., Feillet, F., St-Onge, J., Duffourd, Y., Jugé, C., Roubertie, A., Héron, D., Mignot, C., Raffo, E., et al. (2014). Mutations in SLC13A5 cause autosomal-recessive epileptic encephalopathy with seizure onset in the first days of life. Am. J. Hum. Genet. *95*, 113–120.